

## Supplementary Information

# **In-Situ Generation of Sub-10 nm Silver Nanowires under electron beam irradiation in the TEM**

Junjie Li<sup>\*a,b,c</sup> & Francis Leonard Deepak<sup>\*b</sup>

<sup>a</sup>*CAS Key Laboratory of Functional Materials and Devices for Special Environments, Xinjiang  
Technical Institute of Physics & Chemistry, Chinese Academy of Sciences; Xinjiang Key  
Laboratory of Electronic Information Materials and Devices, 40-1 South Beijing Road, Urumqi  
830011, China*

<sup>b</sup>*Nanostructured Materials Group, International Iberian Nanotechnology Laboratory (INL),  
Avenida Mestre Jose Veiga, Braga 4715-330, Portugal*

<sup>c</sup>*Institute of Materials, School of Engineering, École Polytechnique Fédérale de Lausanne,  
Station 12, CH-1015 Lausanne, Switzerland.*

### **Corresponding Author**

\* Email: [lijunjie@ms.xjb.ac.cn](mailto:lijunjie@ms.xjb.ac.cn) and [leonard.francis@inl.int](mailto:leonard.francis@inl.int)

## EXPERIMENTAL SECTION

**Sample preparation and characterization.** The  $\text{Ag}_2\text{WO}_4$  (AWO) nanorods were synthesized by a wet chemical route<sup>1,2</sup>. X-ray diffraction (XRD) analysis (Figure S1, supplementary information), TEM and high-angle annular dark-field STEM (HAADF-STEM) images (Figure S2, supplementary information) show a successful preparation of AWO nanorods with an orthorhombic structure (JCPDS card no. 34-0061). To fabricate the Ag nanowires on the oxide support, different electron dose rates were attempted and low electron dose rates around 2.0-20.0  $\text{e}/\text{\AA}^2\text{s}$  were adapted in the experiments. In a typical synthesis process, the stoichiometric 2.0 mmol silver nitrate ( $\text{AgNO}_3$ , 99.8%) and 1.0 mmol tungstate sodium dihydrate ( $\text{Na}_2\text{WO}_4 \cdot 2\text{H}_2\text{O}$ , 99.95%) were dissolved separately in 50 mL deionized water. The tungstate sodium dehydrate solution was transferred to a 200 mL glass flask and heated to 90.0 °C under stirring for 15.0 mins. After that, the silver nitrate solution was quickly poured into the hot tungstate sodium dehydrate solution. Accompanied with temperature decrease to  $\sim 70.0$  °C, the suspension of  $\text{Ag}_2\text{WO}_4$  was formed. Subsequently, the suspension was cooled in a beaker with 50.0 mL ice water for 10.0 mins. The resultant white powders were washed with deionized water three times to remove the solvent, and dried at room temperature. X-ray diffraction (XRD) (X'Pert PRO diffractometer, PANalytical), TEM and HAADF-STEM imaging confirm the Chemical composition and morphology of the obtained fine white products.

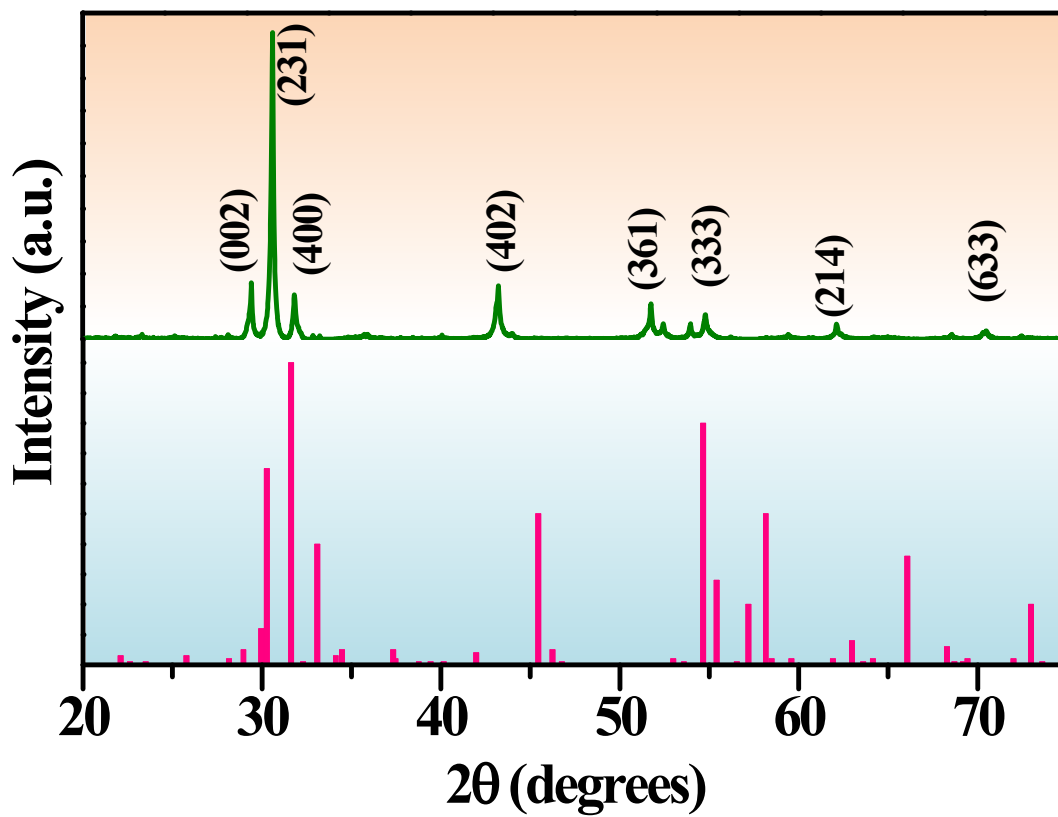
*TEM/STEM observation and EDS analysis:* Under ultrasonication, the obtained fine white powder sample was dispersed in ethanol, and a drop of the white suspension of  $\text{Ag}_2\text{WO}_4$  nanorods was transferred onto  $\text{Si}_3\text{N}_4$  support for the in situ TEM experiments. TEM imaging and EDS mapping were carried out on the Titan Themis TEM equipped with both probe and image Cs corrector and super-X EDS detector at 200 kV, which offered an unprecedented opportunity to probe ultra-small

structures with sub-Ångström resolution. Time sequential TEM images were acquired by Tecnai Imaging and Analysis (TIA) software. The generated Ag nanostructures on the Ag<sub>2</sub>WO<sub>4</sub> surface under irradiation were confirmed by HRTEM images and energy-dispersive X-ray spectroscopy (EDS). The dynamic observations were carried out under TEM mode. The electron dose was changed by tuning the spot size and the size of the electron beam.

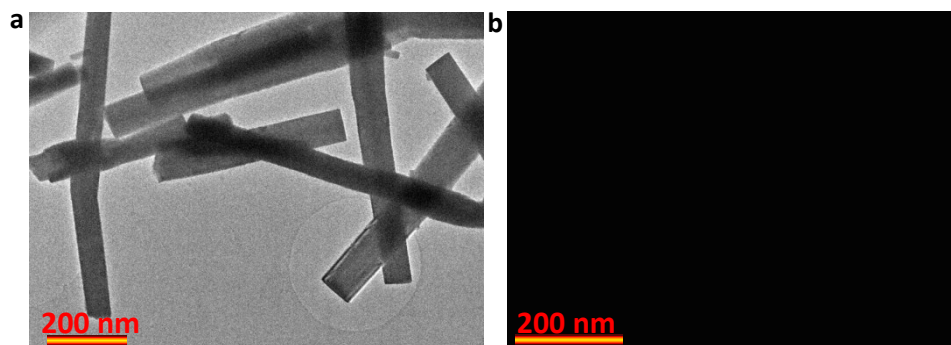
X-ray diffraction (XRD) analysis (Figure S1, supplementary information), TEM and high-angle annular dark-field STEM (HAADF-STEM) images (Figure S2, supplementary information) show a successful preparation of AWO nanorods with an orthorhombic structure (JCPDS card no. 34-0061). To fabricate the Ag nanowires on the oxide support, different electron dose rates were attempted and low electron dose rates around 2.0-20.0 e Å<sup>-2</sup> s<sup>-1</sup> were adapted in the experiments.

## References

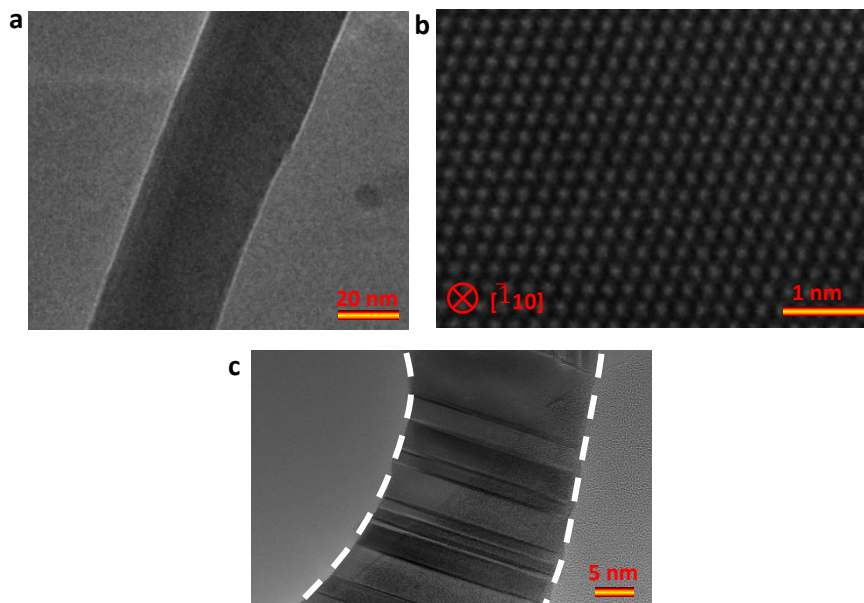
1. Cavalcante, L. *et al.* Cluster coordination and photoluminescence properties of  $\alpha$ -Ag<sub>2</sub>WO<sub>4</sub> microcrystals. *Inorg. Chem.* 2012, **51**, 10675-10687.
2. Li, J., Wang, Z., Li, Y. & Deepak, F. L. In situ atomic-scale observation of kinetic pathways of sublimation in silver nanoparticles. *Adv. Sci.* 2019, **6**, 1802131.



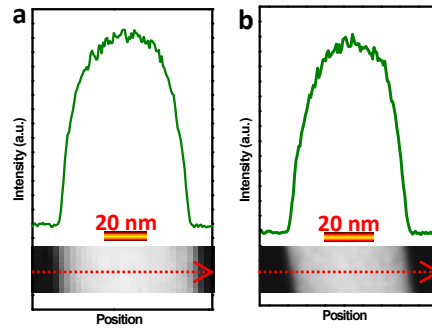
**Supplementary Figure 1.** XRD analysis. XRD results for the synthesized  $\text{Ag}_2\text{WO}_4$  samples and the corresponding standard pattern (JCPDS card no. 34-0061) revealing a successful preparation of pure  $\text{Ag}_2\text{WO}_4$  with an orthorhombic structure.



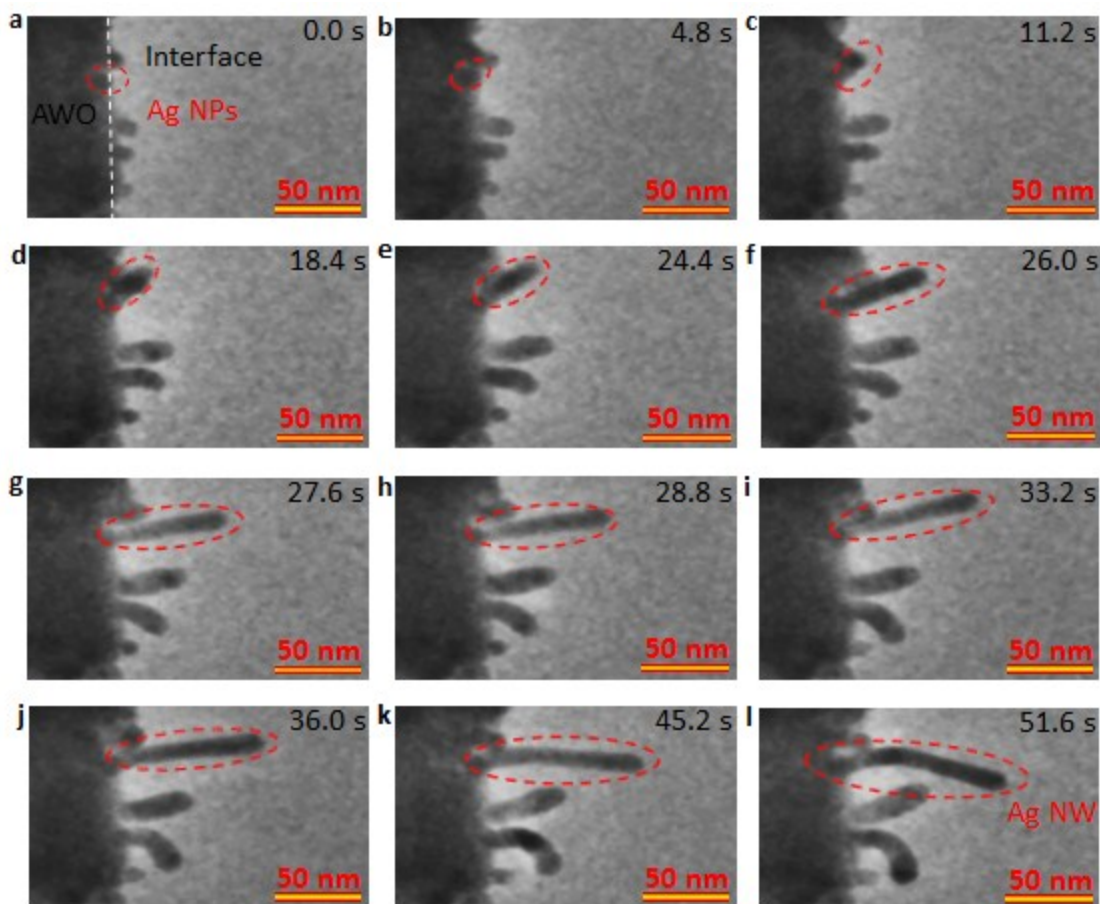
**Supplementary Figure 2.** Morphology of the obtained  $\text{Ag}_2\text{WO}_4$  nanorods. Low magnification TEM (**a**) and HAADF-STEM (**b**) images of the obtained samples.



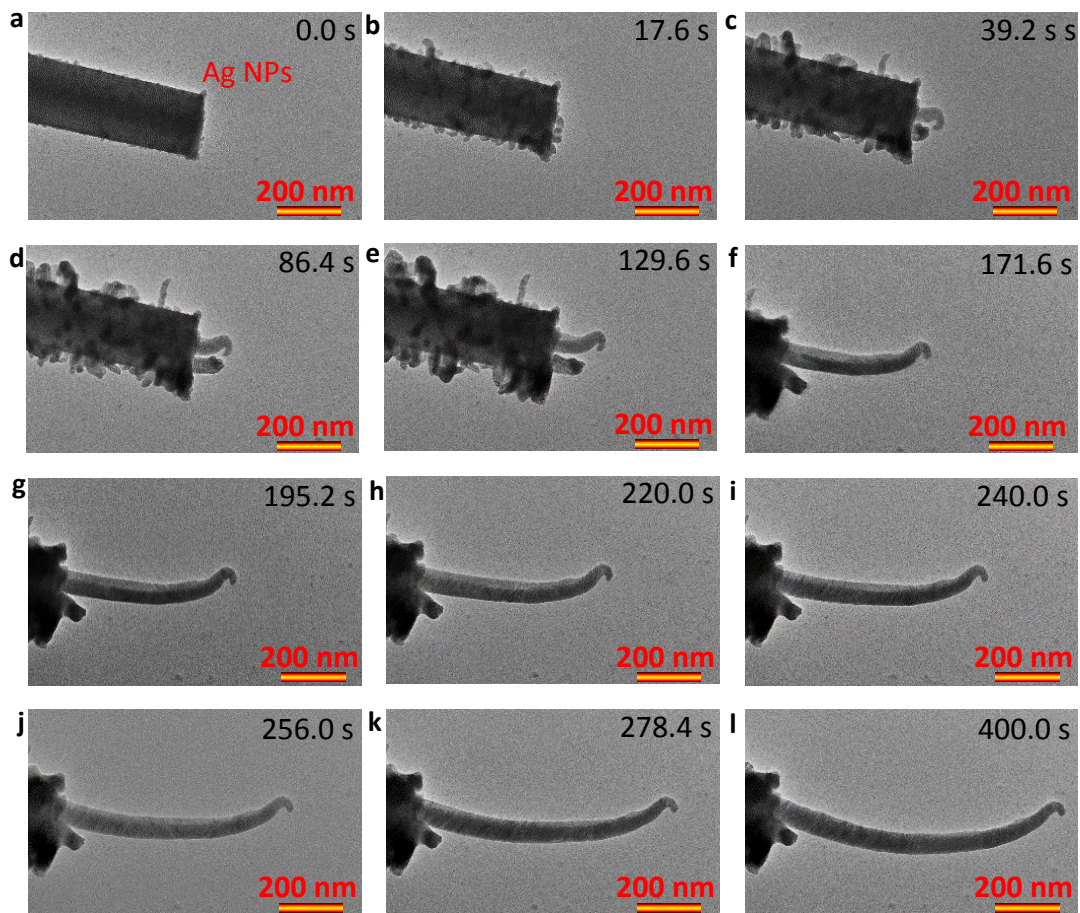
**Supplementary Figure 3.** Morphology and atomic structure of the obtained Ag nanowire. Low magnification TEM (a) and typical high resolution TEM (b) images of the nanowire without the bending region and low magnification TEM (c) image of the bending region in the Ag nanowires.



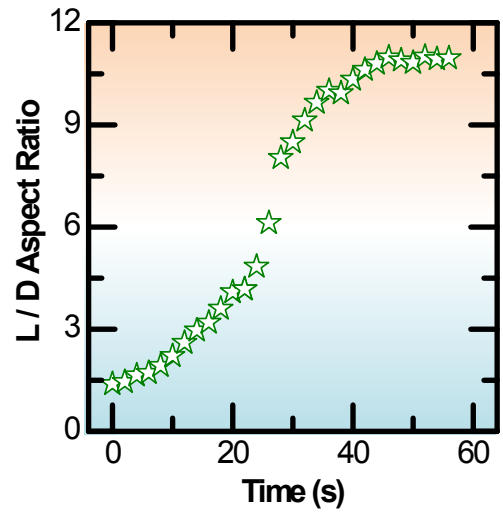
**Supplementary Figure 4.** Intensity profiles show the nanowire structure of the fabricated Ag. a- b, the intensity profiles across the HAADF-STEM images (indicated by the red arrows in the inset HAADF-STEM images) of the formed Ag Nanowires.



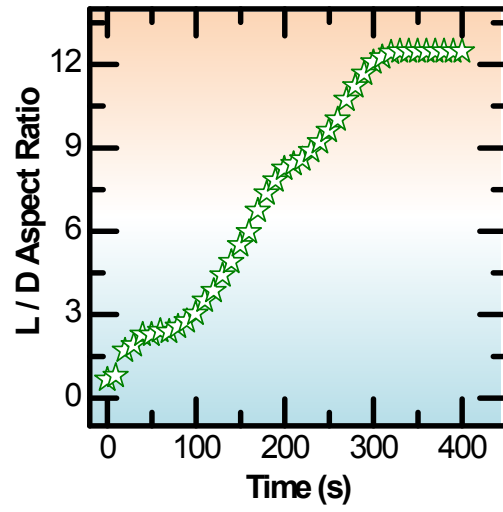
**Supplementary Figure 5. Sequential TEM images showing growth dynamics of the supported sub-10 nm Ag nanowires. a-c, The formation of Ag nanoparticle. d-f, The formation of Ag nanorod. d-f, The growth of nanorod and the formation of Ag nanowires with length/diameter ratio of  $\sim 11$ . The electron dose rate is  $2.0 \text{ e } \text{Å}^{-2} \text{ s}^{-1}$ .**



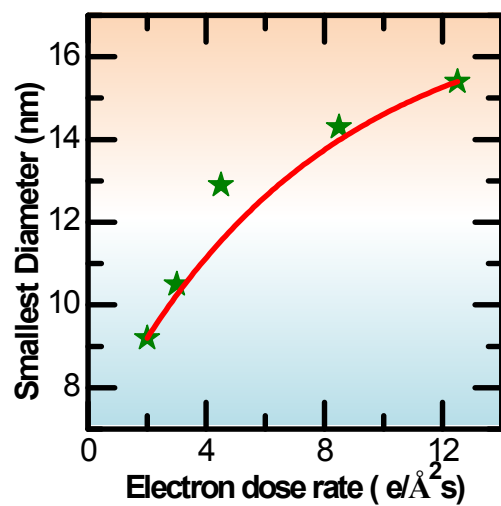
**Supplementary Figure 6.** Sequential TEM images showing growth dynamics of the supported 66.8 nm Ag nanowires. **a-d**, The formation of Ag nanoparticle. **e-i**, The formation of Ag nanorod. **j-l**, The growth of nanorod and the formation of Ag nanowires with length/diameter ratio of  $\sim 11.65$ . The electron dose rate is  $20.0 \text{ e } \text{\AA}^{-2} \text{ s}^{-1}$ .



**Supplementary Figure 7.** Statistical analyses of the length-diameter aspect ratio as a function of time in Video S1.



**Supplementary Figure 8.** Statistical analyses of the length-diameter aspect ratio as a function of time in Video S2.



**Supplementary Figure 9.** Statistical analyses showing the irradiation dose rate-dependent diameter of the formed Ag nanowires under electron beam irradiation.

Table S1. Experimental details for the fabricated Ag nanowires in Figures 1g-n. The value of diameter is measured at the middle of the nanowires.

Figure	Electron dose rate ( $e \text{ \AA}^{-2} \text{ s}^{-1}$ )	Diameter ( $\pm 0.2 \text{ nm}$ )	Length ( $\pm 0.2 \text{ nm}$ )	Length/Diameter $\pm 0.05$	Structure
g	4.5	14.1	15.2	1.08	Nanoparticle
h	8	21.6	20.2	0.94	Nanoparticle
i	4.5	13.8	41.7	3.02	Nanorod
j	3	11.8	89.6	7.59	Nanorod
k	2	9.5	159.8	16.65	Nanowire
l	3	11.2	175.1	15.63	Nanowire
m	12.5	31.6	493.6	15.62	Nanowire
n	20	65.6	818.0	11.65	Nanowire

Table S2. The reported fabrication of Ag nanowires with diameters thinner than 30 nm

The thinnest diameter (nm)	Method	Ref.
25	polyol reduction	3
$20 \pm 2$	polyol reduction	4
20	High pressure synthesis	5
18	polyol reduction	6
$15 \pm 1$	template method	7
13	modified polyol synthesis	8
$9.5 \pm 0.2$	Irradiation-assisted preparation	This work
$6.4 \pm 0.5$	template method	9

### References

- Ran, Y., He, W., Wang, K., Ji, S. & Ye, C. A one-step route to Ag nanowires with a diameter below 40 nm and an aspect ratio above 1000. *Chem. Commun.* 2014, **50**, 14877-14880.
- Li, B., Ye, S., Stewart, I. E., Alvarez, S. & Wiley, B. J. Synthesis and purification of silver nanowires to make conducting films with a transmittance of 99%. *Nano Lett.* 2015, **15**, 6722-6726.
- Lee, E.-J., Chang, M.-H., Kim, Y.-S. & Kim, J.-Y. High-pressure polyol synthesis of ultrathin silver nanowires: Electrical and optical properties. *Appl Mater.* 2013, **1**, 042118.
- Da Silva, R. R. *et al.* Facile synthesis of sub-20 nm silver nanowires through a bromide-mediated polyol method. *ACS nano* 2016, **10**, 7892-7900.
- Hsia, C.-H., Yen, M.-Y., Lin, C.-C., Chiu, H.-T. & Lee, C.-Y. In Situ Generation of the Silica Shell Layer– Key Factor to the Simple High Yield Synthesis of Silver Nanowires. *J. Am. Chem. Soc.* 2003, **125**, 9940-9941.
- Niu, Z. Q., Cui, F., Kuttner E., Xie C. L., Chen, H., Sun, Y. C., Dehestani, A., Schierle-Arndt, K., Yang, P. D., Synthesis of silver nanowires with reduced diameters using benzoin-derived radicals to make transparent conductors with high transparency and low haze. *Nano Lett.* 2018, **18**, 5329-5332.

9. Eisele, D. r. M. *et al.* Photoinitiated growth of sub-7 nm silver nanowires within a chemically active organic nanotubular template. *J. Am. Chem. Soc.* 2010, **132**, 2104-2105.

## **Video Information**

Video S1. The dynamic observations of the growth of the sub-10 nm Ag nanowire. The video was recorded at a ultra-low electron dose rate of  $2.0 \text{ e } \text{Å}^{-2} \text{ s}^{-1}$ , and played at 4 times' normal speed.

Video S2. The dynamic observations of the growth of the 65.6 nm Ag nanowire. The video was recorded at a ultra-low electron dose rate of  $20.0 \text{ e } \text{Å}^{-2} \text{ s}^{-1}$ , and played at 12 times' normal speed.